Contrasting Responses of the Hadley Circulation to Different Meridional SST Structures during the Seasonal Cycle in CMIP5 Models

Juan Feng[1], Yun Chen[1], Jianping Li[1, 2], Yang Li[3], and Yun Yang[1]
[1]*State Key Laboratory of Earth Surface Processes and Resource Ecology and College of Global Change and Earth System Science*, *Beijing Normal University*, *Beijing*, *China*
[2]*Laboratory for Regional Oceanography and Numerical Modeling*, *Qingdao National Laboratory for Marine Science and Technology*, *Qingdao*, *China*
[3]*College of Atmospheric Sciences*, *Chengdu University of Information Technology*, *Chengdu*, *China*

Abstract

The meridional structures of tropical sea surface temperature (SST) play an important role in impacting the variations of Hadley circulation (HC), and the response amplitudes of the HC to different meridional tropical SST structures show contrasting differences. Using the simulations of phase 5 of the Coupled Model Intercomparison Project (CMIP5), the performance of the state-of-art models in reproducing the response contrast of the HC to different SST meridional structures during the seasonal cycle is evaluated in this study. The result indicates that the models show high skills in capturing the climatological features of annual mean HC and tropical SST. Moreover, the leading variabilities of HC and tropical SST during the seasonal cycle are well reproduced for both the equatorially asymmetric and symmetric variations. Furthermore, most of the models display good agreement with the observations in depicting the responses contrast of the HC to different SST meridional structures. These results indicate that the current CMIP5 models show high capability in capturing the response of HC to tropical SST during the seasonal cycle, and provide confidence for further detecting the future variations of HC.

(**Citation**: Feng, J., Y. Chen, J. Li, Y. Li, and Y. Yang, 2017: Contrasting responses of the Hadley circulation to different meridional SST structures during the seasonal cycle in CMIP5 models. *SOLA*, **13**, 102−108, doi:10.2151/sola.2017-019.)

1. Introduction

The meridional distribution of sea surface temperature (SST) plays an important role in impacting the variations of Hadley circulation (HC). It is reported that the alternation of meridional gradient in SST could influence the vertical motion and winds in the lower troposphere (Lindzen and Nigam 1987). Also, the meridional structure of SST could impact the position of boundary layer convergence via adjusting the dynamical and thermal structures of atmosphere (Rind and Rossow 1984). Later work by Hou and Lindzen (1992) further indicated that the location of convergence in the lower troposphere is influenced by the meridional distribution of heating. Our recent research pointed out the position of anomalous convergence in the lower troposphere is subject to the meridional gradient of SST, i.e., the position where the meridional gradient of tropical SST equals zero and changes from negative to positive corresponds to the location of convergence (Feng and Li 2013; Feng et al. 2013). And it is indicated that the meridional variation of SST plays a role in impacting the spatial structure of the anomalous HC (Guo et al. 2016a; Guo and Li 2016). These previous works highlighted the important role of meridional structure of SST on the HC.

Besides the qualitative researches regarding the noticeable impacts of meridional structures of SST on the HC, Feng et al. (2016a) further quantitatively investigate the responses contrast of the HC to different meridional SST structures by decomposing the variations of SST and HC into the equatorially symmetric (SES for SST, and HES for HC) and asymmetric (SEA for SST, and HEA for HC) components. It is found the equatorially asymmetric/symmetric SST structure is accompanied with an anomalous equatorially asymmetric/symmetric HC (Feng et al. 2015, 2016a). And the response amplitude of HEA to SEA is about 5 times to that of the HES to SES even if the magnitudes of SEA and SES are equivalent in the interannual variations (Feng et al. 2016a). This result further ascertains the essential role of meridional structure of SST in determining the variation of HC. On the other hand, given that the HC plays an important role in impacting the global climate variability, it is of interest to further examine whether the role of meridional structures of SST on the HC could be reproduced in the current global Coupled Climate Models (GCMs). As the distinct responses of the HC to different meridional structures of tropical SST may provide a criterion for assessing the performance of the Coupled Model Intercomparison Project Phase 5 (CMIP5) models.

Hu et al. (2013) analyzed changes in the width of the HC based on the CMIP5 models, and indicated that the poleward expansion of HC in CMIP5 is much weaker than the observational reanalyses. As to the intensity of HC, it is reported that a reduction of the annual mean and boreal winter HC strength under global warming in CMIP5 models (Ma et al. 2012; Seo et al. 2014). Feng et al. (2015) found that the bias in reproducing the SST meridional gradient within the Indo-Pacific warm pool is responsible for the unsatisfactory reproduction of long term variability of HC. Guo et al. (2016b) explored the performance of CMIP5 models in reproducing the dominant mode of HC. However, less attention is paid to the performance of the response contrast of HC to different SST meridional structures.

The outputs of the CMIP5 have proved to be a helpful benchmark for assessing model sensitivity and predictability with respect to SST forcing (Taylor et al. 2012; Zheng et al. 2013). In the present study, the ability of the GCMs in reproducing the responses of HC to different SST meridional structures during the annual cycle is focused, and the responses between the observations and models are compared with the aim of assessing the performance of the current state-of-art GCMs.

The remainder of this manuscript is organized as follows. The models, observational datasets, and methodology used in this study are described in Section 2, and the performance of CMIP5 models in reproducing the responses of HC to different meridional SST distributions is illustrated in Section 3. Finally, a discussion and our conclusions are presented in Section 4.

Corresponding author: Juan Feng, State Key Laboratory of Earth Surface Processes and Resource Ecology and College of Global Change and Earth System Science, Beijing Normal University, Beijing, 100875, China.
E-mail: fengjuan@bnu.edu.cn ©2017, the Meteorological Society of Japan.

2. Models, datasets, and methodology

Two monthly-mean atmospheric reanalysis datasets, i.e., the National Centers for Environmental Prediction-Department of Energy Atmospheric Model Intercomparison Project reanalysis covering the period 1979 to the present on a 2.5° × 2.5° grid (NCEP2; Kanamitsu et al. 2002), and the Japanese reanalysis dataset (JRA) that covers 1979 to the present (Onogi et al. 2005) on a 1.25° × 1.25° grid, were used to examine the responses of the HC to different SST meridional structures. The SST reanalysis datasets used were the Extended Reconstructed SST version 3 on a 2° × 2° grid (ERSST; Smith et al. 2008).

We also analyzed the monthly-mean outputs of 16 historical simulations from the CMIP5 models. The models were chosen based upon availability when downloading the data from the Earth System Grid. The relevant details, including the model abbreviations, sources, and horizontal resolutions, are listed in Table 1. More information regarding the experimental design and outputs are available at http://cmip-pcmdi.llnl.gov/cmip5/. Here, only the first simulation (i.e., r1i1p1) is considered because the statistical results obtained are insensitive to the ensemble member analyzed (Taylor et al. 2012; Liu et al. 2016). Due to the availability of the model simulations, the common available period 1979−2004 was used to obtain the climatology for model and observation evaluation, and the annual mean based on this climatology is explored.

The HC is characterized by the mass stream-function (MSF) of the mean meridional circulation. Following Feng et al. (2016a), the spatial variations in SST and HC were separated into two components, i.e., the equatorially symmetric component (HES for HC, SES for SST) and the equatorially asymmetric component (HEA for HC, SEA for SST). Since the MSF is a two-dimension variable, and the value of MSF contains both the magnitude and direction, i.e., the sign of MSF in the Northern Hemisphere and Southern Hemisphere are opposite. The equatorially symmetric (asymmetric) variation of HC here is mainly based on the vertical direction. Accordingly, the HEA and HES can be obtained by:

$$HEA(j) = \frac{MSF(j) + MSF(-j)}{2},$$

$$HES(j) = \frac{MSF(j) - MSF(-j)}{2}.$$

By contrast, SST is a one-dimension variable, thus the SEA and SES are defined as:

$$SEA(j) = \frac{SST(j) - SST(-j)}{2},$$

$$SES(j) = \frac{SST(j) + SST(-j)}{2},$$

where j and $-j$ correspond to the equatorially symmetric meridional locations of the grid points.

EOF analysis was used to determine the leading mode of the variations of SST and the HC during the seasonal cycle after removing the annual mean. The relationship between the HC and SST was investigated using correlation analysis. Spatial correlation was used to examine the similarity of the two variables in the spatial distributions. The regression was calculated using least squares linear regression. The statistical significance of the correlation and regression values was evaluated by means of a two-sided Student's t-test.

3. The performance of the HC to different SST meridional structures in CMIP5

3.1 Simulations in the annual mean HC and SST

First of all, the ability of models in simulating the climatological annual averaged distribution of the HC and zonal mean tropical SST is investigated (Fig. 1). A set of Taylor's diagrams is used to compare the simulation of CMIP5 models and observations (NCEP2 for HC, and ERSST for SST). All of the models show similar features as observed in the climatological HC (Fig. 1a), showing high spatial correlation coefficients with the observations, with all of the coefficients being greater than 0.9. Most of the models display a general amplitude underestimation of the HC, i.e., with a smaller than 1.0 ratio of the standard deviation of the modeled to the observed HC patterns, despite that some models, i.e., CanESM2, CCSM4, CSIR-MK3-6-0, GFDL-ESM2M, and MPI-ESM-LR generate overestimates. As to the tropical SST, although it shows a large disperse in the modeled amplitude comparing with that of the HC, it is seen that all the models well capture the features of climatological tropical zonal mean SST, with high spatial correlations coefficients all greater than 0.85 between the models and observations (Fig. 1b).

In general, all of the models show satisfactory skills in depicting the fundamental characteristics of the climatological annual mean HC and tropical zonal SST. The good reproduction shown above highlights the skills of the CMIP5 models, of which provide

Table 1. Details of the CMIP5 models used in this study.

Model Name	Modeling Center/Country	Horizontal resolution (lon×lat)	Reference
BCC-CSM1-1	Beijing Climate Center, China Meteorological Administration, China	2.81×2.77	Jiang et al. (2010)
BNU-ESM	Beijing Normal University, China	2.81×2.77	Ji et al. (2014)
CanESM2	Canadian Centre for Climate Modelling and Analysis, Canada	2.81×2.79	Chylek et al. (2011)
CCSM4	National Center for Atmospheric Research, USA	1.25×0.9	Gent et al. (2011)
CESM-CAM5	National Science Foundation, Department of Energy, NCAR, USA	1.25×0.9	Neale et al. (2012)
CNRM-CM5	Centre National de Recherches Meteorologiques, Meteo-France, France	1.41×1.40	Voldoire et al. (2013)
CSIRO-Mk3-6-0	Commonwealth Scientific and Industrial Research Organization (CSIRO), Australia	1.875×1.86	Collier et al. (2011)
FGOALs-g2	Institute of Atmospheric Physics, Chinese Academy of Sciences, China	2.81×1.67	Yu et al. (2011)
FIO-ESM	The First Institution of Oceanography, China	2.81×2.81	Qiao et al. (2013)
GFDL-ESM2M	NOAA Geophysical Fluid Dynamics Laboratory, USA	2.5×2.0	Dunne et al. (2013)
HadCM3	Met Office Hadley Centre, UK	3.75×2.5	Gordon et al. (2000)
HadGEM2-ES	Met Office Hadley Centre, UK	1.875×1.25	Martin et al. (2011)
IPSL-CM5A-LR	Institut Pierre Simon Laplace, France	3.75×1.875	Dufresne et al. (2013)
MIROC-ESM	Atmosphere and Ocean Research Institute, National Institute for Environmental Studies and Japan Agency for Marine-Earth Science and Technology, Japan	2.81×1.77	Watanabe et al. (2011)
MPI-ESM-LR	Max Planck Institute for Meteorology, Germany	1.875×1.85	Giorgetta et al. (2013)
NorESM1-M	Norwegian Climate Centre	2.5×1.875	Bentsen et al. (2013)

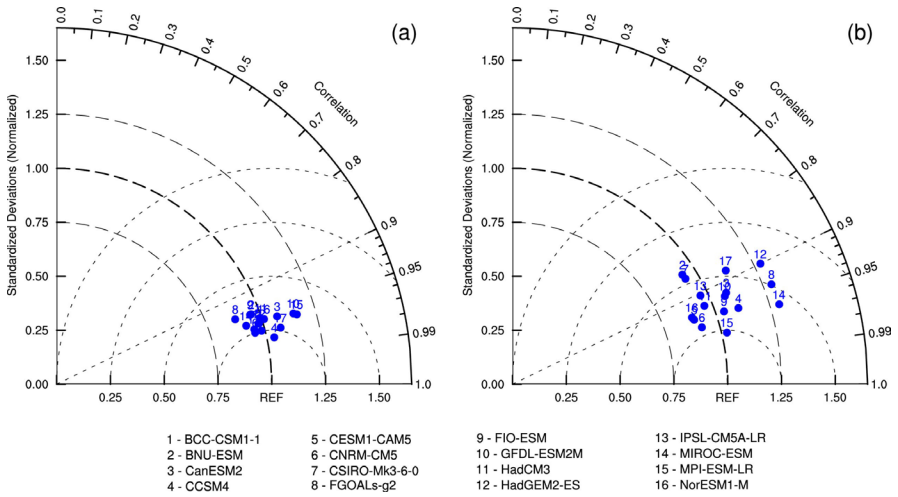

Fig. 1. Taylor diagram of the climatological distribution of annual mean (a) HC and (b) zonal mean SST. The correlation coefficients and ratio of the standard deviation between models and reanalysis data (NCEP2 and ERSST) are shown by the cosine of the azimuth angle and the radial distance, respectively. REF on the horizontal axis indicates the reference point (NCEP2 and ERSST).

the basic guarantee for detecting their performance in reproducing the responses of HC to different SST meridional structures.

3.2 Simulations in the responses contrast of HC to different SST meridional structures

The above discussion was based on the climatological characteristics regarding the annual mean HC and SST, the ability of CMIP5 models in simulating the contrasting responses of HEA and HES to SST is illustrated. Using the method outlined above, we further examined the principal modes of HEA, HES, SEA, and SES based on the observations and CMIP5 outputs, and the spatial distributions of their first principal modes (EOF1) are shown in Figs. 2, 3, 4, and 5, respectively. Only the region 45°S to 45°N is shown considering that the meridional extent of tropical HC appears within this range (Feng et al. 2016b). We see that an equatorially asymmetric mode dominates the variability of the HEA annual cycle, with the explained variance in the range 95.7% to 98.8% (Fig. 2), showing high consistencies with the observations. An equatorially symmetric mode is seen for the variations of HES (Fig. 3), with the explained variance between 58.2% and 75.4%. The coefficients of spatial correlation between the reanalysis dataset and the models in the EOF1 of HEA and HES were in the ranges 0.98−0.99 and 0.71−0.95, respectively (based on the NCEP2 reanalysis).

A similarly effective performance was seen in the variations of the zonal mean SST, which show good consistency with the reanalyses. For example, it shows an approximately linear change in the EOF1 of SEA (Fig. 4), and mirrors the equator for the EOF1 of SES (Fig. 5). The coefficients of spatial correlation between the reanalysis datasets and the models in the EOF1 of SEA and SES were in the ranges 0.98−0.99, and 0.75−0.99 (excepting the CESM1-CAM5 model with a correlation of 0.44), respectively. The correlations of their corresponding PCs are all beyond 0.98 (0.92) for the SEA (SES), and beyond 0.99 (0.80) for the HEA (HES), apart from the correlation of the HES PCs based on the CESM1-CAM5 model and the reanalysis datasets, which is 0.50. This result indicates that both the spatial structure of the EOF1, as well as the seasonal evolution of the PCs based on the reanalyses and models are highly correlated, indicating that the models could well capture the spatial and temporal characteristics of the HC during the seasonal cycle.

Excepting the good agreements in capturing the seasonal cycle of the HC and tropical SST, we see that the performance for the equatorially asymmetric components is better than that for the equatorially symmetric component for both the HC and SST. As reported by Feng and Li (2013), the equatorially symmetric variations of SST are closely associated with the variations of El Niño. This is further verified by the significant correlation between the PC of SES and Niño3 index during 1979−2004 with a coefficient of 0.74 in the interannual scale, indicating that the variations of SES are closely connected with El Niño. In addition, the variation of Niño3 index is accompanied with an anomalous equatorially symmetric meridional circulation, suggesting the variation of HES is linked to El Niño (figure not shown). However, El Niño is not well simulated in the current CMIP models (e.g., Kug et al. 2012; Zhang and Jin 2012), and the results presented here further establish this point.

To this point, the response ratios of HEA with respect to SEA, and HES with respect to SES, based on the models and reanalyses are shown in Fig. 6. First, significant observed positive linkage is seen between that of HEA & SEA (Fig. S1), and HES & SES (Fig. S2), and the response coefficients of HEA to SEA (with a range of 21.33~32.57) is much larger compared to that of HES to SES (with a range of 3.23~11.56). This result implies that all of the models show high capability in capturing the cooperative relation between the tropical SST and HC. As to the response contrast of the HC to different SST meridional structures, we see that some of the models reproduced the contrasting responses as observed in the reanalysis, with a ratio of around four (i.e., BCC-CSM1-1, CanESM2, CNRM-CM5, FGOALs-g2, HadGEM2-ES, MIROC-ESM, and NorESM1-M). However, the HadCM3, CSIRO-Mk3-6-0, and MPI-ESM-LR models overestimated the response contrast of the equatorially asymmetric with respect to the equatorially symmetric components, but the response contrast was underestimated by the BNU-ESM, CESM-CAM5, FIO-ESM, and IPSL-CM5A-LR models.

4. Conclusions and discussion

Based on the simulations of CMIP5 models, the ability of current GCMs in simulating the responses contrast of the HC to different SST meridional structures during the seasonal cycle is evaluated by comparing with the observations. We found that all of the models in this study consistently capture the spatial distribution of the climatological annual mean HC and tropical SST, showing significant spatial correlation coefficients and limited biases in the amplitude between the models and reanalysis. Moreover, the variations of the equatorially asymmetric component are better simulated than those of the equatorially symmetric variations in both the tropical SST and HC. We found that the variations of the SES is closely linked to El Niño, and the variation of the HES is closely related to El Niño (Feng and Li 2013), this indicates a relative ability to simulate El Niño which may induce a lower perfor-

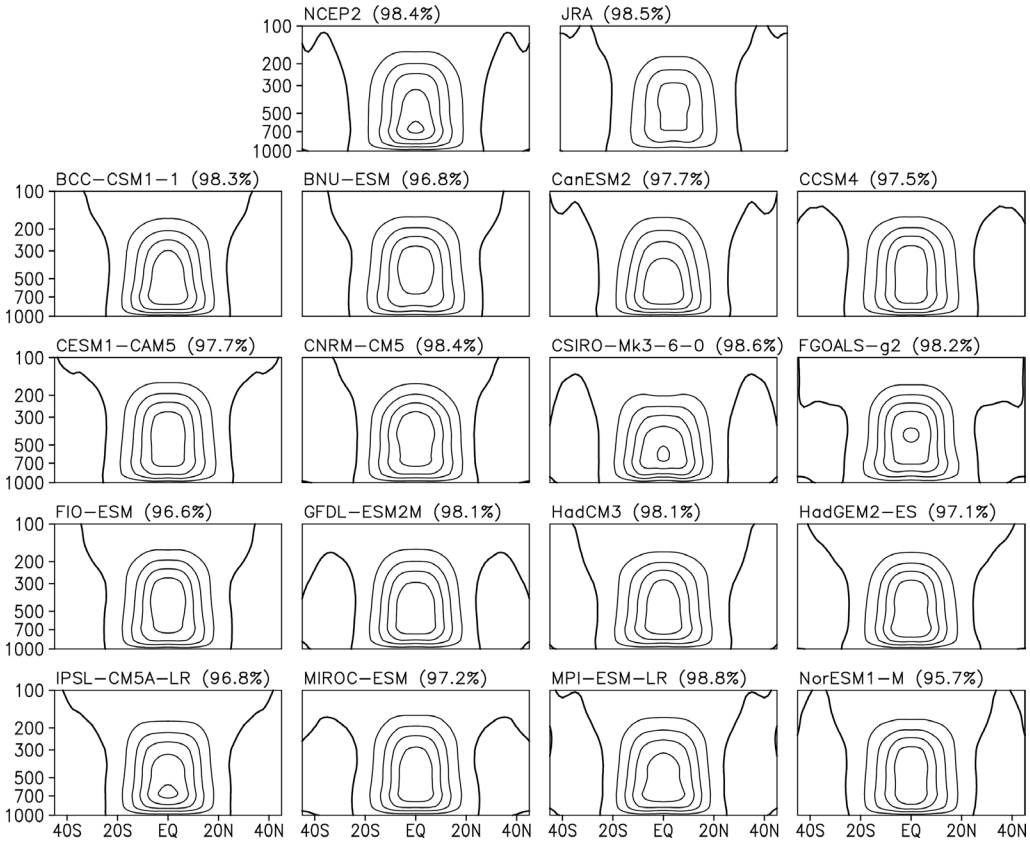

Fig. 2. The EOF1 of the HEA during the seasonal cycle in the observations and CMIP5 models.

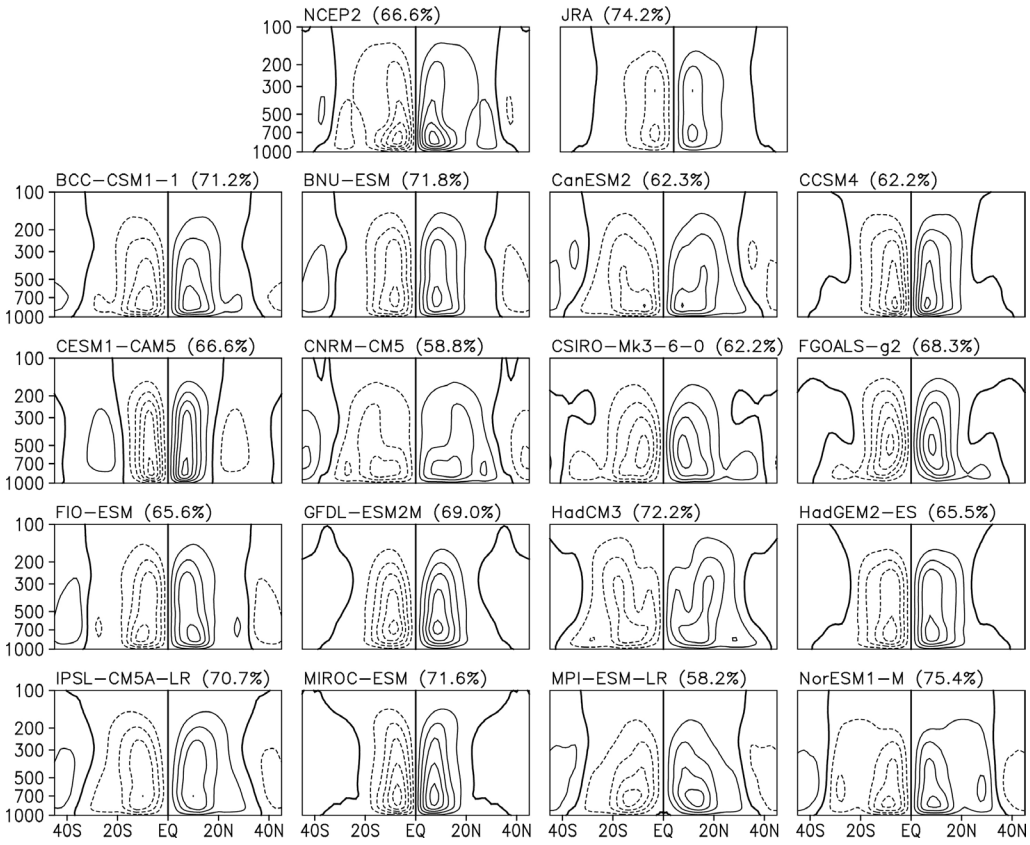

Fig. 3. As in Fig. 2, but for the EOF1 of the HES during the seasonal cycle.

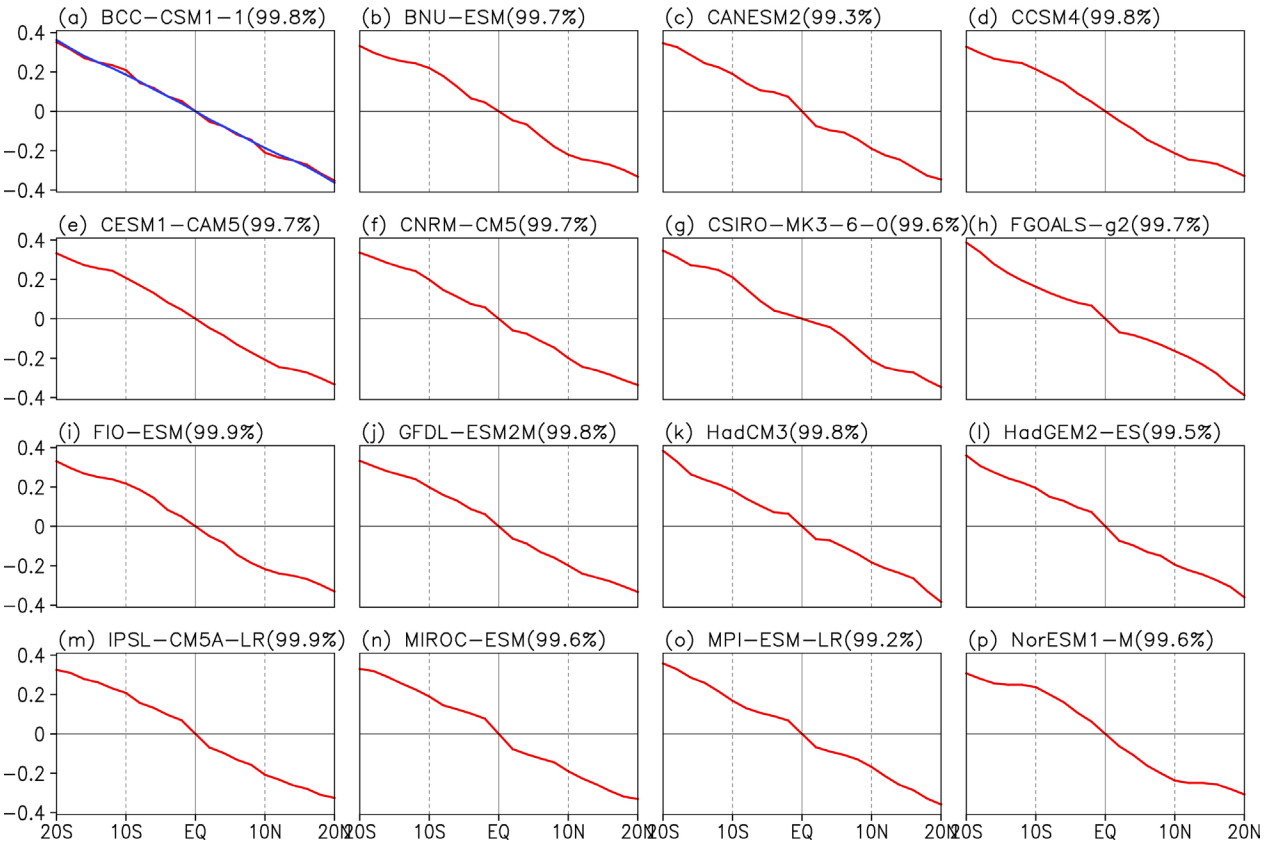

Fig. 4. The EOF1 of the SEA during the seasonal cycle in the observations (blue line) and CMIP5 models (red line).

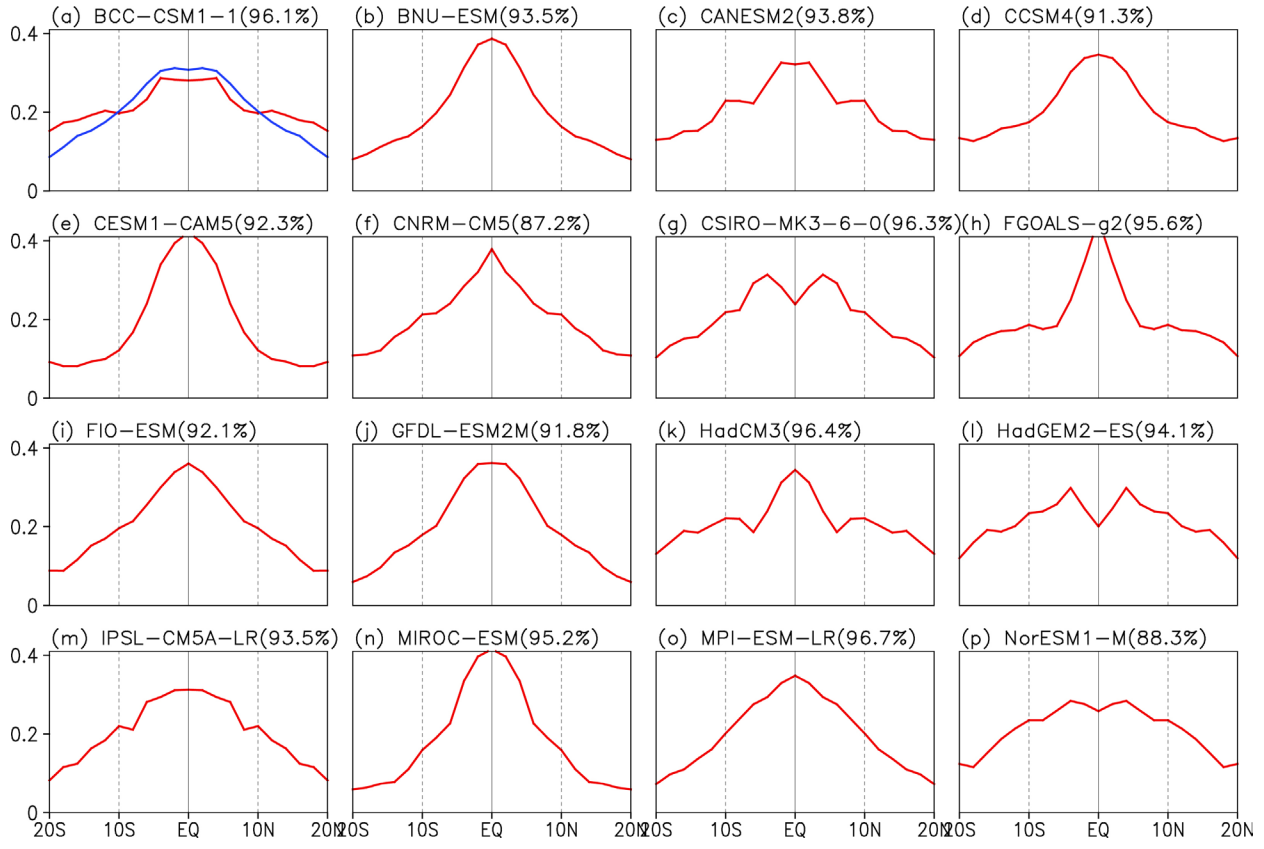

Fig. 5. As in Fig. 4, but for the EOF1 of the SES during the seasonal cycle.

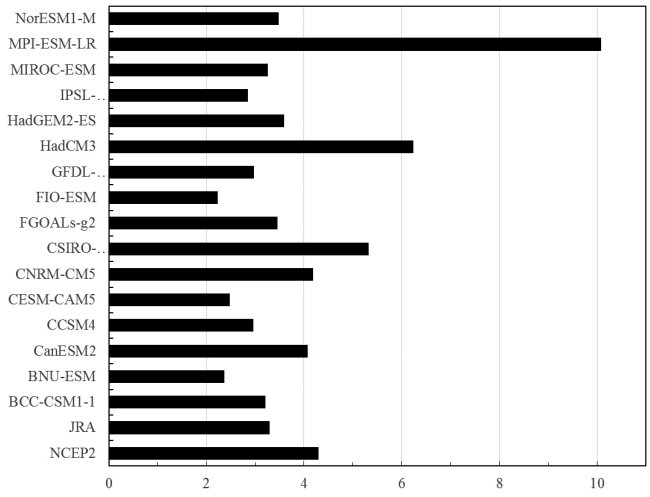

Fig. 6. The ratio distribution of the response of the HEA to SEA with respect to the response of the HES to SES in the observations and CMIP5 models.

mance in HES and SES comparing than HEA and SEA, as has been reported elsewhere (e.g., Guilyardi et al. 2012; Kim and Yu 2012). Furthermore, some of the models are in good agreement with the reanalysis in simulating the differences in the responses between HEA to SEA and HES to SES. However, the responses differences were overestimated in the MPI-ESM-LR, HadCM3, and CSIRO-Mk3-6-0 models, and underestimated in the BNU-ESM, CESM-CAM5, FIO-ESM, and IPSL-CM5A-LR models.

As the HC is the one of the largest meridional circulations, and plays an important role in determining the tropical and extratropical climate, the good performance of the models mentioned above provides a useful tool for further examine whether the responses will alter under future climate scenarios and its variations in the past climate for the availability of long-term outputs of CMIP5 models. These problems will be the focus of future studies.

Moreover, we have explored the performance of the current state-of-art models in reproducing the contrasting responses of HC to different SST meridional structures during the seasonal cycle, however, why the responses of HEA to SEA are times to that of HES to SES is still unknown. Two possible reasons may contribute to the mentioned contrasting responses. Firstly, the meridional gradient associated with SEA and SES are distinct even if their magnitudes are same, and as reported the meridional gradient of SST contributes to the variation of HC (e.g., Lindzen and Nigam 1987; Feng and Li 2013). Secondly, it is of importance to further examine whether the variation of SEA is more likely linked with instability conditions, which may contribute to the large amplitude changes in the HC. However, the reason of the mentioned contrast responses is beyond the scope of the present study, and will be discussed in our future work.

Acknowledgement

This work was jointly supported by the National Natural Science Foundation of China (41475076), Ministry of Science and Technology National Key Research and Development Projects of China (2016YFA0601801), and SOA Program on Global Change and Air-Sea interactions (GASI-IPOVAI-03). The NCEP/DOE and ERSST Reanalysis were obtained from NOAA and are available at http://www.esrl.noaa.gov/psd/data/gridded/. The JRA reanalysis is available online at http://jra.kishou.go.jp/JRA-55/index_en.html. We acknowledge the WCRP's Working Group on Coupled Modelling, which is responsible for CMIP, and the climate modeling groups listed in Table 1 for making the WCRP model outputs available.

Edited by: R. Kawamura

Supplement

Supplement shows the contrast responses of HC to different SST meridional structures based on the CMIP5 models.

Supplemental Figures 1 and 2 show the relationships between the HEA and SEA, and HES and SES, respectively.

References

Bentsen, M., and co-authors, 2013: The Norwegian Earth System Model, NorESM1-M-Part 1: Description and basic evaluation of the physical climate. *Geosci. Model Dev.*, **6**, 687−720.

Chylek, P., and co-authors, 2011: Observed and model simulated 20th century Arctic temperature variability: Canadian Earth System Model CanESM2. *Atmos. Chem. Phys. Discuss*, **11**, 22893−22907.

Collier, M. A., and co-authors, 2011: The CSIRO-Mk3.6.0 Atmosphere-Ocean GCM: Participation in CMIP5 and data publication. *19th International Congress on Modelling and Simulation*, Perth, Australia, 12−16 December 2011 (Available online at http://mssanz.org.au/modsim2011, accessed 10 February 2017).

Dunne, J. P., and co-authors, 2013: GFDL's ESM2 global coupled climate–carbon earth system models. Part II: Carbon system formulation and baseline simulation characteristics. *J. Climate*, **26**, 2247−2267.

Dufresne, J. L., and co-authors, 2013: Climate change projections using the IPSL-CM5 Earth System Model: From CMIP3 to CMIP5. *Climate Dyn.*, **40**, 2123−2165.

Feng, J., and J. P. Li, 2013: Contrasting impacts of two types of ENSO on the boreal spring Hadley circulation. *J. Climate*, **26**, 4773−4789.

Feng, J., J. P. Li, and F. Xie, 2013: Long-term variation of the principal mode of boreal spring Hadley circulation linked to SST over the Indo-Pacific warm pool. *J. Climate*, **26**, 532−544.

Feng, J., and co-authors, 2015: Simulation of the equatorially asymmetric mode of the Hadley circulation in CMIP5 models. *Adv. Atmos. Sci.*, **32**, 1129−1142, doi:10.1007/s00376-015-4157-0.

Feng, J., and co-authors, 2016a: Contrasting responses of the Hadley circulation to equatorially asymmetric and symmetric meridional sea surface temperature structures. *J. Climate*, **29**, 8949−8963.

Feng, J., J. L. Zhu, and F. Li, 2016b: Climatological vertical features of Hadley circulation depicted by the NCEP/NCAR, ERA40, NCEP-DOE, JRA25, EAR-Interim, and CFSR reanalyses. *SOLA*, **12**, 237−241.

Gent, P. R., and co-authors, 2011: The Community Climate System Model version 4. *J. Climate*, **24**, 4973−4991.

Giorgetta, M. A., and co-authors, 2013: Climate and carbon cycle changes from 1850 to 2100 in MPI-ESM simulations for the Coupled Model Intercomparison Project phase 5. *J. Adv. Model Earth Syst.*, **5**, 572−597.

Gordon, C., and co-authors, 2000: The simulation of SST, sea ice extents and ocean heat transports in a version of the Hadley Centre coupled model without flux adjustments. *Climate Dyn.*, **16**, 147−168.

Guilyard, E., and co-authors, 2012: A first look at ENSO in CMIP5. *CLIVAR Exchange*, **17**, 29−32.

Guo, Y. P., and co-authors, 2016: The multidecadal variability of the asymmetric mode of the boreal autumn Hadley circulation and its link to the Atlantic Multidecadal Oscillation. *J. Climate*, **29**, 5625−5641.

Guo, Y. P., J. P. Li, and J. Feng, 2016b: Climatology and interannual variability of the annual mean Hadley circulation in CMIP5 models. *Adv. Climate Change Res.*, **7**, 35−45.

Guo, Y. P., and J. P. Li, 2016: Impact of ENSO events on the interannual variability of Hadley circulation extents in boreal winter. *Adv. Climate Change Res.*, **7**, 46−53.

Hou, A. Y., and R. S. Lindzen, 1992: The influence of concentrated heating on the Hadley circulation. *J. Atmos. Sci.*, **49**, 1233−1241.

Hu, Y. Y., L. J. Tao, and J. P. Liu, 2013: Poleward expansion of the Hadley circulation in CMIP5 simulations. *Adv. Atmos. Sci.*, **30**, 790−795.

Ji, D. Y., and co-authors, 2014: Description and basic evaluation of BNU-ESM version 1. *Geosci. Model Dev. Discuss.*, **7**, 1601−1647.

Jiang, Y., Y. Luo, and Z. C. Zhao, 2010: Projection of wind speed changes in China in the 21st century by climate models. *Chin. J. Atmos. Sci.*, **34**, 323−336.

Kanamitsu, M., and co-authors, 2002: NCEP-DOE AMIP-II Reanalysis (R-2). *Bull. Amer. Meteor. Soc.*, **83**, 1631−1643.

Kim, S. T., and J. Y. Yu, 2012: The two types of ENSO in CMIP5 models. *Geophys. Res. Lett.*, **39**, L11704, doi:10.1029/2012GL052006.

Kug, J. S., Y. G. Ham, J. Y. Lee, and F. F. Jin, 2012: Improved simulation of two types of El Niño in CMIP5 models. *Environ. Res. Lett.*, **7**, 034002, doi:10.1088/1748-9326/7/3/034002.

Onogi., K., and co-authors, 2005: JRA-25: Japanese 25-year reanalysis project-Progress and status. *Quart. J. Roy. Meteor. Soc.*, **131**, 3259−3268.

Lindzen, R. S., and S. Nigam, 1987: On the role of sea surface temperature gradients in forcing low-level winds and convergence in the tropics. *J. Atmos. Sci.*, **44**, 2418−2436.

Liu, T., J. Li, J. Feng, X. F. Wang, and Y. Li, 2016: Cross-seasonal relationship between the boreal autumn SAM and winter precipitation in the Northern Hemisphere in CMIP5. *J. Climate*, **29**, 6617−6636.

Ma, J., S. P. Xie, and Y. Kosaka, 2012: Mechanisms for tropical tropospheric circulation change in response to global warming. *J. Climate*, **25**, 2979−2994.

Martin, G. M., and co-authors, 2011: The HadGEM2 family of Met Office Unified Model climate configurations. *Geosci. Model Dev.*, **4**, 723−757.

Neale, R. B., and co-authors, 2012: Description of the NCAR Community Atmospheric Model (CAM5.0). NCAR TECHNICAL NOTE (Available online at http://www.cesm.ucar.edu/models/cesm1.0/cam/docs/description/cam5_desc.pdf, accessed 10 February 2017).

Qiao, F. L., and co-authors, 2013: Development and evaluation of an Earth System Model with surface gravity waves. *J. Geophys. Res.*, **118**, 4514−4524.

Rind, D., and W. B. Rossow, 1984: The effects of physical processes on the Hadley circulation. *J. Atmos. Sci.*, **41**, 479−507.

Seo, K. H., D. M. Frierson, and J. H. Son, 2014: A mechanism for future changes in Hadley circulation strength in CMIP5 climate change simulations. *Geophys. Res. Lett.*, **40**, 5251−5258, doi:10.1002/2014GL060868.

Smith, T. M., R. W. Reynolds, T. C. Peterson, and J. Lawrimore, 2008: Improvements to NOAA's historical merged land-ocean surface temperature analysis (1880−2006). *J. Climate*, **21**, 2283−2296.

Taylor, K. E., R. J. Stouffer, and G. A. Meehl, 2012: An overview of CMIP5 and the experiment design. *Bull. Amer. Meteor. Soc.*, **93**, 485−498.

Voldoire, A., and co-authors, 2013: The CNRM-CM5.1 global climate model: Description and basic evaluation. *Climate Dyn.*, **40**, 2091−2121.

Watanabe, S., and co-authors, 2011: MIROC-ESM 2010: Model description and basic results of CMIP5-20c3m experiments. *Geosci. Model Dev.*, **4**, 845−872.

Yu, Y. Q., and co-authors, 2011: Versions g1.0 and g1.1 of the LASG/IAP flexible global ocean-atmosphere-land system model. *Adv. Atmos. Sci.*, **28**, 99−117.

Zhang, W. J., and F. F. Jin, 2012: Improvements in the CMIP5 simulations of ENSO-SSTA Meridional width. *Geophys. Res. Lett.*, **39**, L23704, doi:10.1029/2012GL053588.

Zheng, F., J. P. Li, R. Clark, and H. Nnamchi, 2013: Simulation and projection of the Southern Hemisphere Annular Mode in CMIP5 models. *J. Climate*, **26**, 9860−9879.

Manuscript received 10 March 2017, accepted 1 May 2017
SOLA: https://www.jstage.jst.go.jp/browse/sola/